ELSEVIER

Journal of Alloys and Compounds 253–254 (1997) 481–487

Journal of ALLOYS AND COMPOUNDS

Hydrogen adsorption on Pt and Rh electrodes and blocking of adsorption sites by chemisorbed sulfur[1]

A. Zolfaghari, F. Villiard, M. Chayer, G. Jerkiewicz*

Département de chimie, Université de Sherbrooke, Sherbrooke, Québec J1K 2R1, Canada

Abstract

Research on the under-potential deposition of H, UPD H, on Pt and Rh electrodes in aqueous H_2SO_4 solution at temperatures between 273 and 343 K by cyclic-voltammetry followed by theoretical treatment leads to determination of ΔG_{ads}°, ΔS_{ads}° and ΔH_{ads}° and the bond energy between the metal substrate, M, and H_{UPD}, $E_{M-H_{UPD}}$. Knowledge of $E_{M-H_{UPD}}$ results in elucidation of the surface adsorption site of H_{UPD} based on thermodynamic deliberation. The UPD H on Pt is suppressed completely by a monolayer of chemisorbed S, S_{chem}, or partially by a submonolayer of S_{chem} having its surface coverage less than 0.33, $\theta_S < 0.33$. A submonolayer of S_{chem} having $\theta_S = 0.10$ affects ΔG_{ads}°, ΔS_{ads}° and ΔH_{ads}°; the Pt–H_{UPD} bond energy, $E_{Pt-H_{UPD}}$, becomes weaker in presence of the S_{chem} submonolayer. The lateral interactions between H_{UPD} and S_{chem} are brought about by local electron withdrawing effects that propagate through the underlying metal which acts as a mediator.

Keywords: Hydrogen; Electroadsorption; Site blocking; Sulfur; Platinum; Rhodium

1. Introduction

Electrochemical surface science of hydrogen, H, has been undergoing renewed interest due to application of metal–hydride batteries and hydrogen-based fuel cells as power sources for emission-free electric vehicles, EV [1–12]. Hydrogen absorption into host metals can be accomplished either by electrochemical or gas-phase techniques. In electrochemistry, two types of adsorbed H are recognized: (i) the under-potential deposited H, H_{UPD}; and (ii) the over-potential deposited H, H_{OPD} [13]. The species occupy distinct surface adsorption sites and both can undergo entry into the host metal becoming absorbed H, H_{abs} [14]. In the case of charging at negative potentials H absorption and the hydrogen evolution reaction, HER, occur concurrently and the amount of H_{abs} can be related to the overpotential, η, of the HER and the mechanism of the process [15–18]. Certain elements or compounds adsorbed on the metal surface and referred to as site blocking elements, SBE, possess the ability of enhancing or decreasing the H transfer from the adsorbed to the absorbed state [8,17,19–21]. The SBEs reveal a dual action and behave either as surface poisons or as surface promoters depending on their physico–chemical nature [17]. The surface promoters can enhance the rate of H interfacial transfer and increase the amount of absorbed H in the metal, thus increasing its capacity. The latter is of importance to high energy-density M–H batteries which are an alternative to the Ni–Cd ones. Surface poisons which suppress the H interfacial transfer are excellent inhibitors of H embrittlement of metal structures. Experimental evidence indicates that chemical species such as CO, urea, thiourea, compounds of As, Se, S and P are known to affect the adsorption of H in the region corresponding to the under-potential deposition of H, UPD H, and the kinetics of the HER [19–24]. Their action was a subject of thorough theoretical research and numerical simulations based on the lateral interactions between the electroadsorbed H and the coadsorbed SBEs [17]. SBEs affect catalytic properties of the electrified solid–liquid interface through the following action: (i) they can block surface adsorption sites; (ii) they affect energetics of the reaction at the double-layer; (iii) they change the work function of the substrate; (iv) they influence the charge transfer at the electrode–solution interface and (v) they affect adsorption behavior of the reaction products and intermediates. Sulfur, S, is of interest to electrochemical surface science, metal hydride science and technology, and corrosion science because it is a model SBE. The species undergoes strong chemisorption and sustains its chemical identity on the metal electrode surface. Cathodic polariza-

*Corresponding author.

[1]The paper comprises combined results of two conference presentations.

0925-8388/97/$17.00
PII S0925-8388(96)03096-4

tion does not lead to its desorption through formation of a reduced derivative and it can be desorbed only through oxidation at high positive potentials [25,26].

In this paper, the authors present new thermodynamic data the UPD H which lead to elucidation of the surface adsorption sites of H_{UPD} on Pt and Rh electrodes. They present new results on S chemisorption on Pt electrodes and its influence on the UPD H. They determine a relation between the S surface coverage, θ_S, and the coverage by H_{UPD}, $\theta_{H_{UPD}}$. Temperature dependence experimental studies followed by comprehensive theoretical treatment result in determination of ΔG_{ads}°, ΔS_{ads}° and ΔH_{ads}° in absence and presence of S. They evaluate changes of the Pt–H_{UPD} bond energy brought by the S submonolayer.

2. Experimental details

The Pt and Rh electrode preparation procedure and the cell design were described elsewhere [13,24,25,27,28]; the electrode real surface area, A_r is 0.72 ± 0.01 cm^2 for Pt and 0.70 ± 0.01 cm^2 for Rh. The 0.5 M aqueous H_2SO_4 solution was prepared from BDH Aristar grade H_2SO_4 and Nanopure water. The cell was immersed in a water bath fitted with a thermostat (Haake D1). The temperatures, T, in the bath and the cell were controlled by means of thermometers and a K-type thermocouple (80 TK Fluke) and were found to agree to within ±0.5 K. The experimental procedure involved standard cyclic-voltammetry, CV, measurements of the UPD H on Pt and Rh electrodes at T between 273 and 343 K with an interval of 5 K. The instrumentation included: (a) EG&G Model 263A potentiostat–galvanostat; (b) IBM-compatible 80386, 40 MHz computer and (c) EG&G M270 Electrochemical Software. All potentials were measured with respect to the reversible hydrogen electrode, RHE. The potential of the RHE differed from that of the normal hydrogen electrode, NHE, and according to the Nernst equation zero potential on the RHE scale corresponded to -0.021 on the NHE one. Formation of a monolayer of chemisorbed S, S_{chem}, on Pt was accomplished by electrode immersion in 0.01 M aqueous Na_2S (Aldrich) solution for 300 s followed by rinsing in Nanopure water. Appraisal of influence of S_{chem} on the H adsorption behavior was accomplished by recording CV profiles in the potential regions corresponding to UPD H and the surface oxide formation.

3. Results and discussion

3.1. Temperature dependence and thermodynamics of the UPD H

Fig. 1 shows a series of CV adsorption–desorption for the UPD H on Pt and Rh from 0.5 M aqueous H_2SO_4 solution for temperature between 273 and 343 K with an interval of 10 K recorded at the sweep rate of 20 mV s^{-1} (experiments were conducted with an interval of 5 K but in order not to obscure the graphs fewer experimental curves are shown). The CVs recorded on Pt and Rh electrodes manifest differences in the shape and number of the adsorption–desorption peaks; they shift towards less-positive potentials upon T increase and they are symmetric with respect to the potential axis indicating reversibility of the process. An increase of the cathodic current at the lower potential limit of the CVs is due to the onset of the over-potential deposition of H, OPD H. The UPD H adsorption–desorption behavior may be summarized as follows: T increase does not result in new CV features and the UPD H adsorption–desorption CVs shift towards less-positive values. Theoretical treatment of the experimental data based on Eq. (1) allows determination of the Gibbs free energy of adsorption, $\Delta G_{ads}^{\circ}(H_{UPD})$, as a function of the H_{UPD} surface coverage, $\theta_{H_{UPD}}$, and T thus 3D $\Delta G_{ads}^{\circ}(H_{UPD})$ versus ($\theta_{H_{UPD}}$, T) plots [14,24].

$$\frac{\theta_{H_{UPD}}}{1-\theta_{H_{UPD}}} = P_{H_2}^{1/2} \exp\left(-\frac{EF}{RT}\right) \exp\left(-\frac{\Delta G_{ads}^{\circ}(H_{UPD})}{RT}\right) \quad (1)$$

where $\Delta G_{ads}^{\circ}(H_{UPD})$ includes a H_{UPD} coverage-dependent

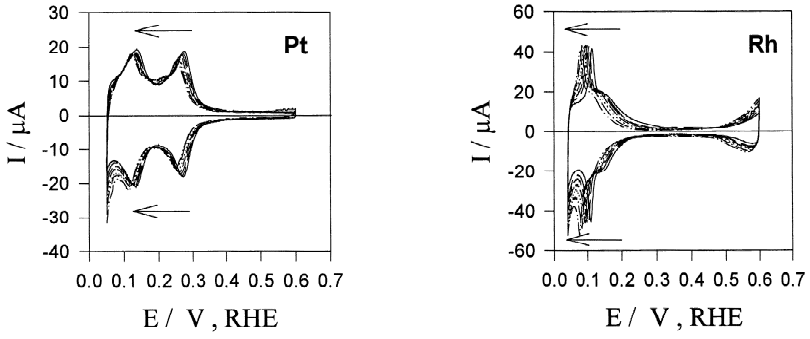

Fig. 1. Series of CV profiles for the UPD H on Pt and Rh electrodes in 0.5 M aqueous H_2SO_4 solution for a temperature range between 273 and 343 K, with an interval of 10 K; the sweep rate $s=20$ mV s^{-1}, the arrows indicate shift of the adsorption–desorption peaks upon the temperature increase.

parameter, $\omega(\theta_{H_{UPD}})$, which describes lateral interactions, thus $\Delta G_{ads}^{\circ}(H_{UPD})_{\theta_{H_{UPD}}\neq 0} = \Delta G_{ads}^{\circ}(H_{UPD})_{\theta_{H_{UPD}}=0} + \omega(\theta_{H_{UPD}})$, $P_{H_2}^{1/2}$ is the partial pressure of H_2 in the reference electrode compartment, E is the potential measured versus the RHE and R and F are physico–chemical constants. The results of these calculations are shown in Fig. 2 and they indicate that in the case of Pt $\Delta G_{ads}^{\circ}(H_{UPD})$ has values from -25 to -12 kJ mol^{-1} and in case of Rh $\Delta G_{ads}^{\circ}(H_{UPD})$ has values from -17 to -8 kJ mol^{-1}, thus the driving force of the UPD H on Pt is greater than in the case of Rh. In both cases $\Delta G_{ads}^{\circ}(H_{UPD})$ has the most-negative values at the lowest T and the smallest $\theta_{H_{UPD}}$. For a given T, $\Delta G_{ads}^{\circ}(H_{UPD})$ increases with $\theta_{H_{UPD}}$ indicating that the lateral interactions between the H_{UPD} adatoms are of the repulsive nature [29–32]. The slope of the $\Delta G_{ads}^{\circ}(H_{UPD})$ versus $\theta_{H_{UPD}}$ plots is a measure of the strength of the repulsions and it may be concluded (Fig. 2) that they are stronger in the case of H_{UPD} adatoms on Pt than on Rh. The $\Delta G_{ads}^{\circ}(H_{UPD})$ versus T relations for a given $\theta_{H_{UPD}}$ are linear and allow determination of the entropy of adsorption, $\Delta S_{ads}^{\circ}(H_{UPD})$, based on Eq. (2):

$$\Delta S^{\circ}_{ads}(H_{UPD}) = -\left[\frac{\partial \Delta G^{\circ}_{ads}(H_{UPD})}{\partial T}\right]_{\theta_{H_{UPD}}=const} \quad (2)$$

The data shown in Fig. 3 indicate that $\Delta S_{ads}^{\circ}(H_{UPD})$ has values from -80 to -41 J mol^{-1} K^{-1} for Pt and from -126 to -29 J mol^{-1} K^{-1} for Rh. In the case of Pt, the $\Delta S_{ads}^{\circ}(H_{UPD})$ versus $\theta_{H_{UPD}}$ relation reveals two maxima which are associated with the two CV peaks whereas in the case of Rh $\Delta S_{ads}^{\circ}(H_{UPD})$ increases monotonously. The enthalpy of adsorption, $\Delta H_{ads}^{\circ}(H_{UPD})$, is determined based on the experiment values of $\Delta G_{ads}^{\circ}(H_{UPD})$ and $\Delta S_{ads}^{\circ}(H_{UPD})$ and the well-known formula $\Delta G^{\circ} = \Delta H^{\circ} - T\Delta S^{\circ}$. The results shown in Fig. 4 demonstrate that $\Delta H_{ads}^{\circ}(H_{UPD})$ has values from -46 to -27 kJ mol^{-1} for Pt and from -52 to -21 kJ mol^{-1} for Rh. Knowledge of $\Delta H_{ads}^{\circ}(H_{UPD})$ allows evaluation of the bond energy be-

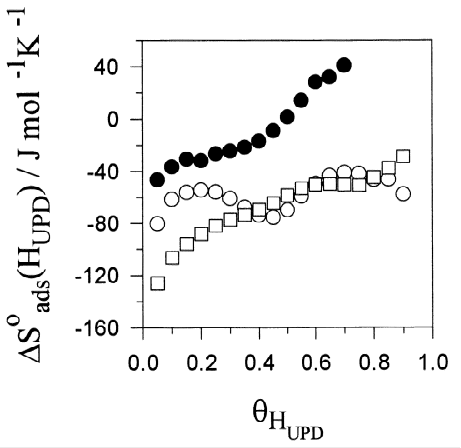

Fig. 3. $\Delta S_{ads}^{\circ}(H_{UPD})$ versus $\theta_{H_{UPD}}$ relations for the UPD H from 0.5 M aqueous H_2SO_4 on: (i) Pt in absence of S_{chem} (○); (ii) Rh in absence of S_{chem} (□); and (iii) Pt in presence of S_{chem}, $\theta_S = 0.1$, (·).

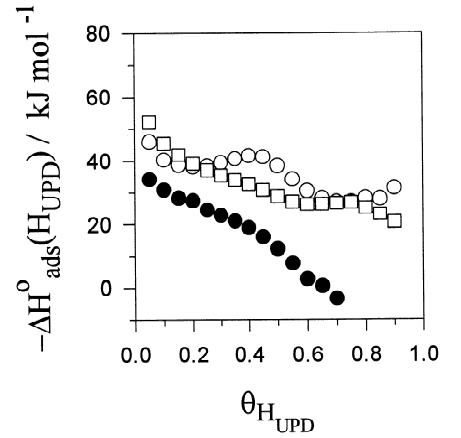

Fig. 4. $\Delta H_{ads}^{\circ}(H_{UPD})$ versus $\theta_{H_{UPD}}$ relations for the UPD H from 0.5 M aqueous H_2SO_4 on: (i) Pt in absence of S_{chem} (○), (ii) Rh in absence of S_{chem} (□); and (iii) Pt in presence of S_{chem}, $\theta_S = 0.1$, (·).

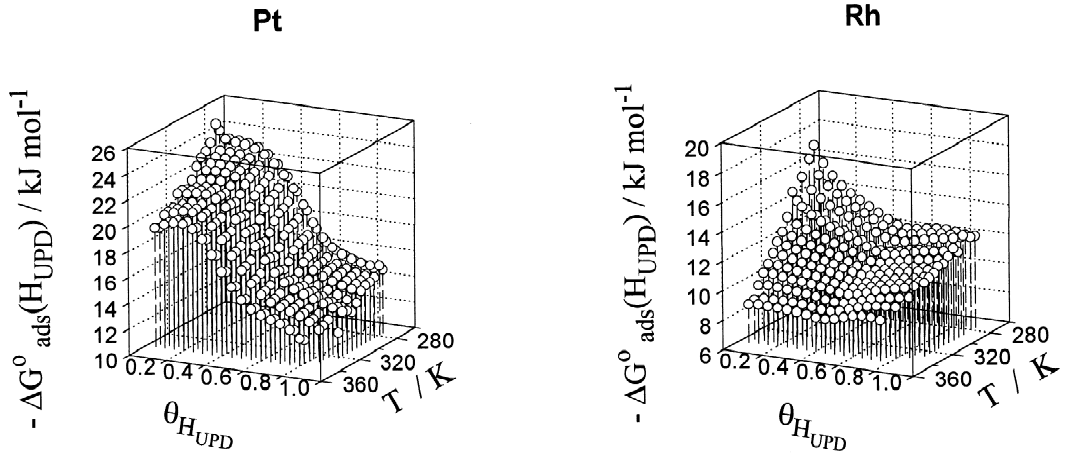

Fig. 2. 3D plots showing $\Delta G_{ads}^{\circ}(H_{UPD})$ versus $\theta_{H_{UPD}}$ and T for the UPD H on Pt and Rh electrodes in 0.5 M aqueous H_2SO_4.

tween the substrate, M (here M is Pt or Rh), and H_{UPD}, $E_{M-H_{UPD}}$, based on Eq. (3):

$$E_{M-H_{UPD}} = \frac{1}{2}D_{H_2} - \Delta H^{\circ}_{ads}(H_{UPD}) \quad (3)$$

where D_{H_2} is the dissociation energy of the hydrogen molecule and $D_{H_2} = 436$ kJ mol^{-1}. Such determined values of $E_{Pt-H_{UPD}}$ and $E_{Rh-H_{UPD}}$ as a function of $\theta_{H_{UPD}}$ are shown in Fig. 5 and they demonstrate that $E_{Pt-H_{UPD}}$ varies from 245–264 kJ mol^{-1} and those of $E_{Rh-H_{UPD}}$ from 239–270 kJ mol^{-1}. The values of $E_{Pt-H_{UPD}}$ and $E_{Rh-H_{UPD}}$ fall close to those for the bond energy between Pt or Rh and chemisorbed H, H_{chem}, which are $243 \leq E_{Pt-H_{chem}} \leq 255$ kJ mol^{-1} and $E_{Rh-H_{chem}} = 255$ kJ mol^{-1}, respectively [33]. Proximity of these indicates that H_{chem} and H_{UPD} are thermodynamic equivalent species. Subsequently, if M–H_{UPD} and M–H_{chem} bond energies are close to each other, then it is rational to conclude that H_{UPD} occupies the same surface adsorption site as H_{chem} thus that it is embedded in the surface lattice of the metal substrate.

3.2. Sulfur chemisorption on Pt electrodes

A layer of chemisorbed S, S_{chem}, on Pt was formed by its immersion in 0.01 M aqueous Na_2S solution. The surface coverage of the S_{chem} layer was 1.2 with respect to the electrode real surface area; it exceeded unity because the electrode was of polycrystalline nature and more S_{chem} atom were adsorbed at the grain boundaries and surface imperfections resulting in the S/Pt ratio greater than one. This layer of S_{chem} suppressed completely the UPD H on Pt [19,20] as it was revealed by CV measurements (Fig. 6). Coupled FTIR, AES, CEELS and electrochemical measurements [25,26,34,35] indicate that S_{chem} is in its atomic form. The S_{chem} layer can be removed by Pt cycling into the oxide formation region [36,37], thus the surface

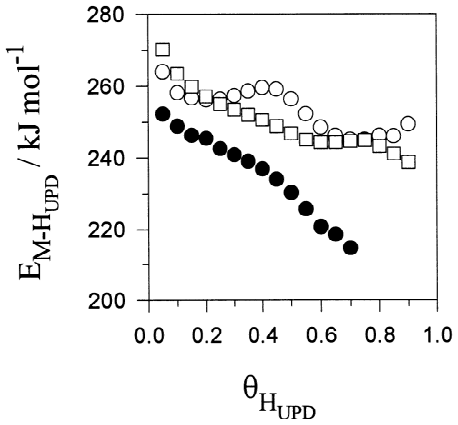

Fig. 5. E-{ {FUNC {M-H-{UPD}}} } versus $\theta_{H_{UPD}}$ relations for the UPD H from O.5 M aqueous H_2SO_4 on: (i) Pt in absence of S_{chem} (○); (ii) Rh in absence of S_{chem} (□); and (iii) Pt in presence of S_{chem}, $\theta_S = 0.1$, (·).

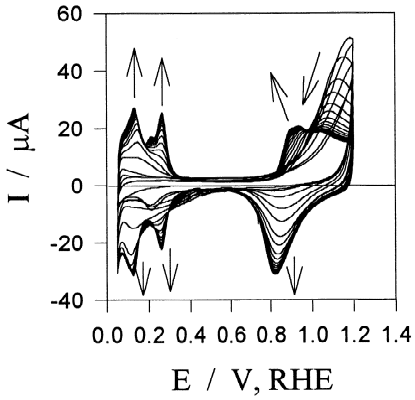

Fig. 6. Series of CV profiles for Pt electrode covered with a layer of S_{chem} in O.5 M aqueous H_2SO_4 solution at 298 K; the sweep rate $s = 20$ mV s^{-1}. Upon potential cycling to 1.20 V, RHE, the S_{chem} layer undergoes oxidative desorption; unblocked surface sites become available to H_{UPD}. Presence of S_{chem} also affects the surface oxidation of Pt.

oxidation and the S_{chem} oxidative desorption overlap. Complete removal of the S_{chem} layer cannot be accomplished within one CV and it requires several cycles (Fig. 6). FTIR and UHV data [25,26,38] indicate that the S_{chem} oxidative desorption at $E \leq 1.1$ V, RHE, results in formation of sulfate and its desorption:

$$S_{chem} + 4H_2O \overset{E \geq 1.1\ V}{\rightarrow} SO_4^{2-} + 8H^+ + 6e \quad (4)$$

Because the Pt oxidation commences at 0.85 V, RHE, and the S_{chem} oxidative desorption at $E \leq 1.1$ V, RHE, the total anodic charge equals $q_{AN(i)} = q_{OX(i)} + q_{S(i)}$ ($q_{OX(i)}$ is the oxide charge, $q_{S(i)}$ is the charges of S_{chem} desorption; the subscript i represents the ith cycle). The cathodic charge $q_{CATH(i)}$, at $0.5 \leq E \leq 1.2$ V, RHE, corresponds to reduction of the surface oxide [35]. Their difference for every CV allows one to evaluate the charge of the sulfur oxidative desorption per cycle, $q_{S(i)}$. Summation of these charges for all CVs leads to determination of the overall charge of the S_{chem} oxidative desorption, $q_S = \Sigma q_{S(i)}$, and when divided by the number of electrons transferred during the oxidation, it results in the total number of S_{chem} adatoms on the Pt electrode prior to the oxidative desorption.

$$N_S = \frac{q_S}{6e} \quad (5)$$

An analysis of the CVs (Fig. 6) allows one to establish a relation between the H_{UPD}, S_{chem} and oxide coverages, $\theta_{H_{UPD}}$, θ_S and θ_O, respectively, with respect to the number of cycles for the S_{chem} oxidative desorption (Fig. 7). Examination of the results leads to three observations: (i) less than 1 ML of S_{chem}, is required for complete suppression of the UPD H; (ii) the $\theta_{H_{UPD}}$ and θ_S relations intersect at the coverage of 0.33 and (iii) presence of S_{chem} suppresses the Pt oxidation. The authors examined the effectiveness of the S_{chem} desorption by Pt cycling to

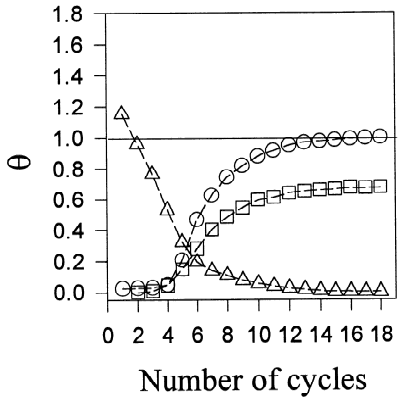

Fig. 7. Relation between the H_{UPD} surface coverage, $\theta_{H_{UPD}}$ (○), the S_{chem} surface coverage, θ_S (△), the surface oxide coverage, θ_O (□), and the number of respective cycles to 1.2 V for S_{chem} oxidative desorption determined on the basis of results presented in Fig. 6.

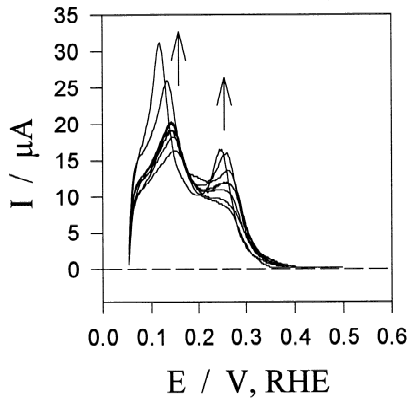

Fig. 8. Series of the CV profiles for the UPD H on Pt electrode in 0.5 M aqueous H_2SO_4 solution in presence of a S_{chem} submonolayer ($\theta_S = 0.1$) for a temperature range between 273 and 343 K, with an interval of 10 K; the sweep rate $s = 20$ mV s^{-1}. The arrows indicate changes in the profile brought about by T increase.

potentials higher than 1.2 V and they found that potential limits higher than 1.2 V results in more effective removal of the S_{chem} layer [35]. Formation of a ML of S_{chem} followed by cycling to $E = 1.2$ V results in a submonolayer of S_{chem} whose coverage can be controlled with the accuracy of some 2% of a ML especially in the range of $\theta_S \leq 0.4$.

3.3. Thermodynamics of the UPD H at Pt in presence of a submonolayer of chemisorbed S

The main idea behind the project was assessment of the influence of S_{chem} on thermodynamics of the UPD H and the bond Pt–H_{UPD} energy. The authors presumed that S_{chem} adatoms (a submonolayer), coadsorbed with H_{UPD}, can withdraw electron density from the Pt atoms to which S_{chem} is bonded. This electron withdrawal gives rise to a localized electron deficit which is compensated by withdrawing electron density from the neighboring Pt atoms and those involving the Pt–H_{UPD} bond [17,35]. The Pt substrate acts as a mediator bringing about lateral S_{chem}–H_{UPD} interactions. Hence, the electron density of the Pt–H_{UPD} bond should be decreased by the coadsorbed S_{chem}, thus the Pt–H_{UPD} bond should be weaker in presence of S_{chem} that in its absence. This concept was tested experimentally and theoretically and the results are presented below.

A submonolayer of S_{chem} ($\theta_S = 0.1$) on Pt was formed according to the procedure described above. CVs for the UPD H on Pt in O.5 M aqueous H_2SO_4 solution at T between 273 and 343 K with an interval of 10 K at the sweep rate of 20 mV s^{-1} are shown in Fig. 8. The results indicate that $\theta_{H_{UPD}}$ is strongly affected by T variation and presence of S_{chem}. The Gibbs free energy of adsorption in presence of S_{chem}, $\Delta G_{ads(S)}^{\circ}(H_{UPD})$, is evaluated on the basis of Eq. (6) and the results shown in Fig. 9 [17].

$$\frac{\theta_{H_{UPD}}}{1-\theta_{H_{UPD}}-\theta_S} = P_{H_2}^{1/2}\exp\left(\frac{EF}{RT}\right)\exp\left(-\frac{\Delta G^{\circ}_{ads(S)}(H_{UPD})}{RT}\right) \quad (6)$$

In presence of S_{chem}, $\Delta G_{ads(S)}^{\circ}(H_{UPD})$ varies from -22 to -9 kJ mol^{-1}, thus it has values less negative than those in absence of S_{chem}. In the analysis of the $\Delta G_{ads}^{\circ}(H_{UPD})$ versus $\theta_{H_{UPD}}$ plots for $T = \text{const}$ (Fig. 2), it has been mentioned that the lateral interactions between H_{UPD} adatoms are repulsive [24,29–33]. In the case of the UPD H in presence of S_{chem}, the changes of $\Delta G_{ads(S)}^{\circ}(H_{UPD})$ with $\theta_{H_{UPD}}$ are more pronounced at low T than at high T whereas in absence of S_{chem} they are roughly the same. Thus in presence of S_{chem} the lateral repulsions between the H_{UPD} adatoms are stronger at low T than at high T. The entropy of adsorption in presence of S_{chem}, $\Delta S_{ads(S)}^{\circ}(H_{UPD})$, was evaluated based on Eq. (2); it has

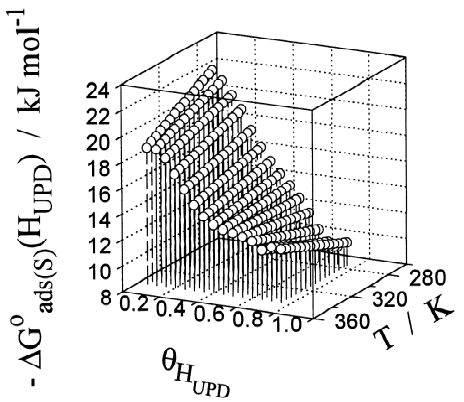

Fig. 9. 3D plots showing the Gibbs free energy of the UPD H, $\Delta G_{ads(S)}^{\circ}(H_{UPD})$, versus $\theta_{H_{UPD}}$ and T, for adsorption in presence of a S_{chem} submonolayer ($\theta_S = 0.1$) from 0.5 M aqueous H_2SO_4.

values from -46 to 41 J mol^{-1} K^{-1} (Fig. 3). The results show that $\Delta S_{ads(S)}^{\circ}(H_{UPD})$ varies from negative values at low $\theta_{H_{UPD}}$ to positive ones at high $\theta_{H_{UPD}}$ thus indicating an increase of $\Delta S_{ads(S)}^{\circ}(H_{UPD})$ with $\theta_{H_{UPD}}$. Comparison of $\Delta S_{ads}^{\circ}(H_{UPD})$ with $\Delta S_{ads(S)}^{\circ}(H_{UPD})$ reveals that presence of S_{chem} increases the entropy of the UPD. The enthalpy of adsorption in presence of S_{chem}, $\Delta H_{ads(S)}^{\circ}(H_{UPD})$, is determined based on the $\Delta G_{ads(S)}^{\circ}(H_{UPD})$ and $\Delta S_{ads(S)}^{\circ}(H_{UPD})$ values. The results shown in Fig. 4 demonstrate that $\Delta H_{ads(S)}^{\circ}(H_{UPD})$ has values from -34 to 3 kJ mol^{-1}. An analysis of the data indicates that presence of S_{chem} increases the enthalpy of adsorption with respect to its values in absence of S_{chem}. Determination $\Delta H_{ads(S)}^{\circ}(H_{UPD})$ allowed evaluation of the influence of presence of S_{chem} on the Pt–H_{UPD} bond energy, $E_{Pt-H_{UPD}(S)}$. The values of $E_{Pt-H_{UPD}(S)}$ for various $\theta_{H_{UPD}}$ were evaluated according to Eq. (3) and they vary from 214–252 kJ mol^{-1} (Fig. 5). The results demonstrate that presence of S_{chem} decreases the Pt–H_{UPD} bond energy by some 12–31 kJ mol^{-1}, depending on $\theta_{H_{UPD}}$. The decrease of the Pt–H_{UPD} bond energy indicates that the S_{chem} adatoms create an electron deficit at the Pt–H_{UPD} bond giving rise to a weaker Pt–H_{UPD} bond.

The authors believe that the results represent an important contribution to comprehension of the atomic-level mechanism of the action of SBEs and their impact on coadsorbed H_{UPD} adatoms and that they will serve in subsequent development of criteria for selection and design of surface species which could act selectively either as surface poisons or surface poisons of H adsorption and absorption.

4. Conclusions

1. Immersion of Pt in aqueous Na_2S solution leads to formation of a ML of S_{chem} which suppresses the UPD H; a submonolayer of S_{chem} having its coverage less than 0.33 partially blocks the UPD H. The S_{chem} ML can be gradually removed by oxidative desorption at $E=1.2$ V and the S_{chem} coverage can be controlled with precision of 2% of a ML.

2. Summary of thermodynamic data for the studied systems

State function versus system	$\Delta G_{ads}^{\circ}(H_{UPD})$ (kJ mol^{-1})	$\Delta S_{ads}^{\circ}(H_{UPD})$ (J mol^{-1} K^{-1})	$\Delta H_{ads}^{\circ}(H_{UPD})$ (kJ mol^{-1})	E_{M-HUPD} (kJ mol^{-1})
H_{UPD} on Pt	-25–-12	-80–-41	-46–-27	245–264
H_{UPD} on Rh	-17–-8	-126–-29	-52–-21	239–270
H_{UPD} on Pt in presence of S_{chem} ($\theta_S=0.1$)	-22–-9	-46–41	-34–3	214–252

3. The S_{chem} adatoms adsorbed on Pt create an electron deficit at the Pt surface atoms to which they are bonded. This deficit propagates through the Pt substrate and gives rise to electron withdrawal from the Pt–H_{UPD} bond, thus to a weaker Pt–H_{UPD} bond.

4. The H_{UPD} adatoms have repulsive lateral interactions which become stronger in presence of the S_{chem} submonolayer than in its absence.

Acknowledgments

Acknowledgment is made to the NSERC of Canada and le FCAR du Québec for support of this research project. A. Zolfaghari gratefully acknowledges a graduate fellowship from the MCHE of Iran. F. Villiard and M. Chayer conducted this research as their last term projects.

References

[1] K.M. Mackay, *Hydrogen Compounds of the Metallic Elements*, E. and F.N. Spon, London, 1966.
[2] G. Alefeld and J. Volkl, (eds.), *Hydrogen in Metals*, Parts I and II, Springer–Verlag, New York, 1978.
[3] L. Schlapbach, (ed.), *Hydrogen in Intermetallic Compounds*, Part I, Springer–Verlag, New York, 1988; Part II, Springer–Verlag, New York, 1992.
[4] P.K. Subramanyan, in J.O'M. Bockris, B.E. Conway, E. Yeager and R.E. White (eds.), *Comprehensive Treatise of Electrochemistry*, Vol. 4, Plenum Press, New York, 1981, Ch. 8.
[5] J.J.G. Willems, *Ph.D. Thesis*, Eindhoven, The Netherlands, 1984.
[6] A.F. Andersen and A.J. Maeland (eds.), *Hydrides for Energy Storage*, Pergamon Press, Oxford, 1978.
[7] B.E. Conway and G. Jerkiewicz, (eds.), *Electrochemistry and Materials Science of Cathodic Hydrogen Absorption and Adsorption*, The Electrochemical Society, PV 94–21, Pennington, NJ, 1995.
[8] R.A. Oriani, J.P. Hirth and M. Smialowski (eds.), *Hydrogen Degradation of Ferrous Metals*, Noyes Publications, Park Ridge, NJ, 1985.
[9] S.R. Ovshinsky, M.A. Fetcenko and J. Ross, *Science, 260* (1993) 176.
[10] S.R. Ovshinsky, K. Sapru, B. Reichman and A. Reger, US Patents No. 4623 597 (1986); see also S.R. Ovshinsky and M.A. Fetcenko, US Patent No. 5096 667, 1992; No. 5104 617, 1992; No. 5135 589, 1992; No. 5238 756, 1993; No. 5277 999, 1994.
[11] M. Ciureanu, D. Moroz, R. Ducharme, D.H. Ryan, J. Ström-Olsen and M. Tirudeau, *Zeit. Phys. Chem. Bd., 183* (1994) 365; Q.M. Yang, M. Ciureanu, D.H. Ryan and J. Ström-Olsen, *J. Electrochem. Soc., 141* (1994) 2108; 2113; 141 (1994) 2430.
[12] O. Savadogo, P.R. Roberge and T.N. Veziroglu (eds.), *New Materials for Fuel Cell Systems* 1, Proceedings of the First International Symposium on New Materials for Fuel Cell Systems, Édition de l'École Polytechnique de Montréal, Montréal, 1995.
[13] B.E. Conway and L. Bai, *J. Chem. Soc., Faraday Trans. 1* 81 (1985) 1841.
[14] G. Jerkiewicz and A. Zolfaghari, *J. Electrochem. Soc., 143* (1996) 1240.
[15] B.E. Conway and G. Jerkiewicz, *J. Electroanal. Chem., 357* (1993) 47.
[16] B.E. Conway and G. Jerkiewicz, *Z. Phys. Chem. Bd., 183* (1994) 281.
[17] G. Jerkiewicz, J.J. Borodzinski, W. Chrzanowski and B.E. Conway, *J. Electrochem. Soc., 142* (1995) 3705.

[18] A. Lasia and D. Grégoire, *J. Electrochem. Soc., 142* (1995) 3393.
[19] P. Marcus and E. Protopopoff, *Surface Sci., 161* (1985) 533; *Surface Sci. Letters, 169* (1986) L237; *J. Vac. Sci. Technol., A5* (1986) 944.
[20] E. Protopopoff and P. Marcus, *J. Electrochem. Soc., 135* (1988) 3073; *J. Chim. Phys., 88* (1991) 1423; *C. R. Acad. Sci. Paris, t. 308, Série II* (1989) 1685.
[21] J. McBreen, *J. Electroanal. Chem., 287* (1990) 279.
[22] S. Morin and B.E. Conway, *J. Electroanal. Chem., 376* (1994) 135.
[23] D. Zurawski, K. Chan and A. Wieckowski, *J. Electroanal. Chem., 210* (1986) 315; see also D. Zurawski and A. Wieckowski, *Langmuir, 8* (1992) 2317.
[24] G. Jerkiewicz and A. Zolfaghari, *J. Phys. Chem., 100* (1996) 8454.
[25] C. Quijada, A. Rodes, J.L. Vázquez, J.M. Pérez and A. Aldaz, *J. Electroanal. Chem., 394* (1995) 217.
[26] C. Quijada, A. Rodes, J.L. Vázquez, J.M. Pérez and A. Aldaz, *J. Electroanal. Chem., 398* (1995) 105.
[27] H. Angerstein-Kozlowska, B.E. Conway and W.B.A. Sharp, *J. Electroanal. Chem., 43* (1973) 9.
[28] H. Angerstein-Kozlowska, in E. Yeager, J.O'M. Bockris, B.E. Conway and S. Sarangapani (eds.), *Comprehensive Treatise of Electrochemistry*, Vol. 9, Plenum Press, New York, 1984, Ch. 9.
[29] I. Langmuir, *J. Am. Chem. Soc., 40* (1918) 1361.
[30] R.H. Fowler and F.A. Guggenheim, *Statistical Thermodynamics*, Cambridge University Press, London, 1939.
[31] A.W. Adamson, *Physical Chemistry of Surfaces*, John Wiley and Sons, New York, 1990.
[32] G.A. Somorjai, *Introduction to Surface Chemistry and Catalysis*, John Wiley and Sons, New York, 1994.
[33] K. Christman, *Surface Sci. Rep., 9* (1988) 1.
[34] Y.-E. Sung, W. Chrzanowski, A. Zolfaghari, G. Jerkiewicz and A. Wieckowski, *J. Am. Chem. Soc*., in press, 1996.
[35] A. Zolfaghari, G. Jerkiewicz, Y.-E. Sung and A. Wieckowski, in K. Itaya and A. Wieckowski (eds.), *Electrode Processes* VI, The Electrochemical Society, PV 96–8, Pennington, NJ, 1996.
[36] G. Tremiliosi-Filho, G. Jerkiewicz and B.E. Conway, *Langmuir, 6* (1992) 658.
[37] G. Jerkiewicz, G. Tremiliosi-Filho and B.E. Conway, *Electroanal. Chem., 344* (1992) 359.
[38] N. Batina, J.W. McCargar, L. Laguren-Davidson, C.-H. Lin and A. T. Hubbard, *Langmuir, 5* (1989) 123.